

Elementary fractal geometry.

5. Weak separation is strong separation

Christoph Bandt
 Mathematical Institute
 University of Greifswald, Germany
 bandt@uni-greifswald.de

Michael F. Barnsley
 Mathematical Sciences Institute
 Australian National University, Canberra
 Michael.Barnsley@anu.edu.au

April 9, 2024

Abstract

For self-similar sets, there are two important separation properties: the open set condition and the weak separation condition introduced by Zerner, which may be replaced by the formally stronger finite type property of Ngai and Wang. We show that any finite type self-similar set can be represented as a graph-directed construction obeying the open set condition. The proof is based on a combinatorial algorithm which performed well in computer experiments.

1 Overview

A self-similar set is a nonempty compact subset A of \mathbb{R}^d which is the union of shrunk copies of itself, as defined by Hutchinson's equation

$$A = \bigcup_{f \in F} f(A) . \quad (1)$$

Here F denotes a finite set of contractive similarity mappings, called an iterated function system or IFS. The set F fulfils the open set condition (OSC) if there exist an open set $U \subset \mathbb{R}^d$ such that

$$\bigcup_{f \in F} f(U) \subset U \quad \text{is a disjoint union of subsets of } U . \quad (2)$$

This definition was introduced 1946 by Moran [42] to show that the Hausdorff measure with respect to the similarity dimension α is positive on A . It turned out to be the appropriate condition for many geometric studies of A . The OSC says that the intersections $f(A) \cap g(A)$ with f, g in F , or in the generated semigroup

$$F^* = \bigcup_{k=0}^{\infty} F^k \quad \text{with } F^k = \{f_1 f_2 \cdots f_k \mid f_j \in F\}$$

are small: they are contained in the boundary of an open set. In algebraic terms, the OSC states that the IFS is discrete in the following sense [8]. There is a neighborhood V of the identity map id in the space of similitudes which does not contain maps of the form $f^{-1}g$ with $f, g \in F^*$. For details see Chapter 4 in the recent book [12] and [6, 10, 17].

Many examples of self-similar sets admit ‘exact overlaps’ in the sense that $f(A) = g(A)$ for some $f, g \in F^*$. Zerner [54] noted that such coincidences of pieces, which obviously contradict the OSC, do not change the discrete character of the IFS. The weak separation condition (WSC) is satisfied if there is a neighborhood V of id which does not contain maps of the form $f^{-1}g$ with $f, g \in F^*$, except for id itself. In one dimension, Lau and Ngai [35] studied this concept in a measure-theoretic setting.

Zerner proved that self-similar sets with WSC have positive Hausdorff measure in some dimension β which is smaller than the similarity dimension. While OSC needs to be checked, weak separation is satisfied for large classes of IFS; for example in the cases of crystallographic data [54] and complex Pisot expansion factors [6]. Ngai and Wang [43] defined a finite type property which implies weak separation [44], and gave an explicit formula for β . All known examples with WSC, and a large class of one-dimensional examples fulfil the finite type condition [25, 30], cf. [12, Section 4.3]. There are many recent studies on WSC attractors and their measures [19, 20, 22, 26, 29, 32, 45, 50, 53].

Here we show that weak separation is just a variant of the OSC. So in principle, there exists only one type of separation. More precisely, we prove that finite overlap type self-similar sets are graph-directed constructions [40], abbreviated graph IFS or GIFS [15, 21], with the open set condition. The basic idea is to cut away the overlaps by going from an IFS to a GIFS.

To simplify the presentation, we assume that all similitudes $f \in F$ have the same contraction factor r , that is $|f(x) - f(y)| = r|x - y|$ for all points $x, y \in \mathbb{R}^d$. We assume that the IFS has *finite overlap type*: there are only finitely many maps $h = f^{-1}g$ with $f, g \in F^k$ for some k , such that $A \cap h(A)$ contains a whole piece $f'(A)$ for some $f' \in F^*$. Compared with the literature [12, 25, 30, 43], this is the weakest possible finite type condition. It is exactly the condition which Ngai and Wang needed when they gave their more complicated definition [6, Section 2]. Finite overlap type implies WSC [44], and all known examples with WSC have finite overlap type. It is expected that the two properties coincide, which was proved for certain one-dimensional cases by Feng [25] and Hare, Hare and Rutar [30].

The GIFS in this paper have a simple form: a system of equations of the form 1 for n attractors $B_k \subseteq A$ instead of the single attractor A .

$$B_k = \bigcup_{f \in F_k} f(B_{j(f,k)}) \quad \text{for } k = 1, \dots, n. \quad (3)$$

Here $F_k \subseteq F$ so all equations involve only similitudes from F . We can consider j as a map $j : \bigcup_{k=1}^n F_k \times \{k\} \rightarrow \{1, \dots, n\}$ which just means that each equation contains specific attractors B_j for the maps $f \in F_k$. This GIFS fulfils the OSC if there exist open sets $U_k, k = 1, \dots, n$ such that

$$\bigcup_{f \in F_k} f(U_{j(f,k)}) \subset U_k \quad \text{is a disjoint union of subsets of } U_k \text{ for } k = 1, \dots, n. \quad (4)$$

Theorem 1 *Let F be an IFS of similitudes on \mathbb{R}^d , each with the same scaling factor, with the finite overlap type property. Let the attractor (self-similar set) be A . Then F can be extended to a GIFS of the form (3) with the OSC and $B_k \subseteq A$.*

This result goes beyond Hausdorff dimension, which can be easily determined from GIFS with the OSC [40]. The theorem shows that attractors with weak separation have the same structure as those with the OSC: they have a quite homogeneous modular structure consisting of pieces of positive Hausdorff measure in the respective dimension.

The GIFS will be explicitly constructed. The method was implemented on a computer. In the last part of the paper we handle new two-dimensional WSC examples of moderate complexity while the literature so far has been focussed on one-dimensional attractors [12, 25, 30, 43]. Treating self-similar sets of even larger complexity is a challenge concerning both the computer implementation and the mathematical problem of minimising the number of equations in a GIFS.

Finite automata play the main part in this paper. They have been around in dynamical systems and fractal geometry for many years, without explicit mention. Finite type shifts and sofic shifts are automata-generated symbolic data [37, Chapter 3]. “The concept of a ‘sophic system’ is simply the ergodic theorist’s specialized name for what is known in other branches of science as a finite state automaton” [24, Preface]. A ‘graph-directed construction’ [40] or GIFS is the addressing of fractal attractors by such automata-generated symbolic data. A ‘neighbor graph’ [6, 7, 11] or ‘overlap graph’ addresses the dynamical boundary, or the overlaps, by automata-generated symbols. In automata-theoretic terms, the construction of this paper describes a transducer from the overlap automaton of a WSC attractor to a GIFS automaton of OSC attractors. This means that our approach to WSC does not depend on similitudes. It can also be realized in an affine, conformal or topological setting, cf. [7, 32, 50]. Moreover, our computer experiments in Section 10 lead to questions of automata theory.

We start with two simple examples illustrating the basic idea. In Section 3 we introduce the overlap graph as our main tool. Section 4 compares this method with that of Ngai and Wang. The GIFS construction is presented in Section 5 and worked out for an example. The proof of the OSC for Theorem 1 in Section 6 uses an idea of Schief [47] and the concept of a central open set [9]. Detailed examples in Sections 7 and 8 and results of computer experiments in Sections 9 and 10 show that our method works well for fractals and tiles of moderate complexity.

All fractal figures in this paper were produced by Mekhontsev’s IFStile package [41]. Overlap graphs were treated with MATLAB. The first named author gratefully acknowledges an encouraging e-mail conversation with Dylan Thurston.

2 The basic idea

Figure 1 shows the only two-dimensional example of Ngai and Wang [43, Example 5.4], reproduced in [12, Example 4.3.7]. Our approach works although not all maps have the same factor. The overlapping attractor $A = f_1(A) \cup f_2(A) \cup f_3(A)$ is generated by the IFS

$$f_1(x, y) = (t^2x, t^2y + t), \quad f_2(x, y) = (tx + t^2, ty), \quad f_3(x, y) = (tx, ty) \quad \text{with } t = \frac{1}{2}(\sqrt{5} - 1). \quad (5)$$

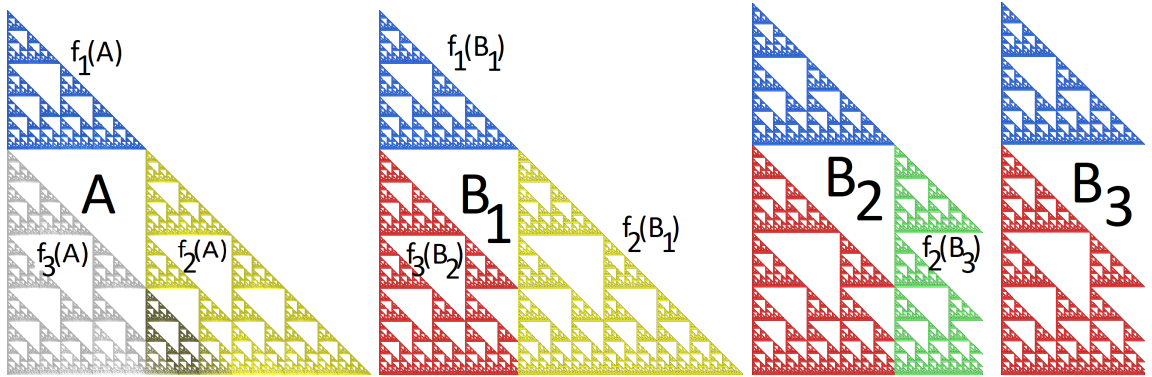


Figure 1: The example of Ngai and Wang and an associated non-overlapping GIFS.

We eliminate the overlap in the leftmost part of Figure 1 by introducing copies B_k of A with cut-away overlaps. Let $B_1 = A$ with a non-overlapping representation. We replace the left part $f_3(B_1)$ of B_1 by $f_3(B_2)$ where B_2 is chosen so that $f_3(B_2)$ (drawn in red) and $f_2(B_1)$ touch each other within a vertical line segment. Actually, B_2 is the closure of $B_1 \setminus f_3^{-1}f_2(B_1)$. Now B_2 is a union of three pieces $f_1(B_1)$, $f_3(B_2)$ and $f_2(B_3)$ where B_3 (drawn in green) is a new set smaller than B_2 . Finally, $B_3 = B_2 \cap f_2^{-1}(B_2)$ is the union of only two pieces, and we obtain the GIFS

$$B_1 = f_1(B_1) \cup f_2(B_1) \cup f_3(B_2), \quad B_2 = f_1(B_1) \cup f_2(B_3) \cup f_3(B_2), \quad B_3 = f_1(B_1) \cup f_3(B_2). \quad (6)$$

The IFS (5) together with the equations (6) determine the GIFS. We did not calculate anything. We just looked at the structure of the overlap. This combinatorial approach will work in general.

The dimension β of the B_k can be obtained from (6) by the method of Mauldin and Williams [40]. For the present example there is a simpler trick. We know that the β -dimensional Hausdorff measure μ is positive and finite, and for a similitude f with factor t we have $\mu(f(E)) = t^\beta \mu(E)$. We can assume $\mu(A) = 1$ and write $s = t^\beta$ so that $\mu(f_2(A)) = \mu(f_3(A)) = s$ and $\mu(f_1(A)) = s^2$. The second and third piece overlap in a piece of third level so that $\mu(f_2(A) \cap f_3(A)) = s^3$. The measure of A is the sum of the measure of the pieces $f_j(A)$ minus the measure of the overlap: $1 = s^2 + s + s - s^3$. The root in $[0, 1]$ is $s \approx 0.445$, which implies $\beta = \frac{\log s}{\log t} \approx 1.682$, simplifying the calculation in [12, 43].

This was essentially a one-dimensional example, with f_2 as dummy variable for better visualization. The proper golden triangle in Figure 2 was introduced by Sidorov et al. [18] where the dimension was calculated with an infinite IFS. In the complex plane, the IFS of the symmetric golden triangle can be written as

$$f_1(z) = tz + tv, \quad f_2(z) = tz + t, \quad f_3(z) = tz \quad \text{with } v = \frac{1}{2}(1 + i\sqrt{3}) \text{ and } t = \frac{1}{2}(\sqrt{5} - 1). \quad (7)$$

In establishing the GIFS we follow the principle that each point should be represented by its smallest address with respect to the lexicographic order of the pieces [14]. Thus $B_1 = A$, but B_2 must be reduced so that $f_1(B_1)$ and $f_2(B_2)$ do not overlap. From B_3 we have to subtract two overlaps corresponding to two neighbors with smaller index.

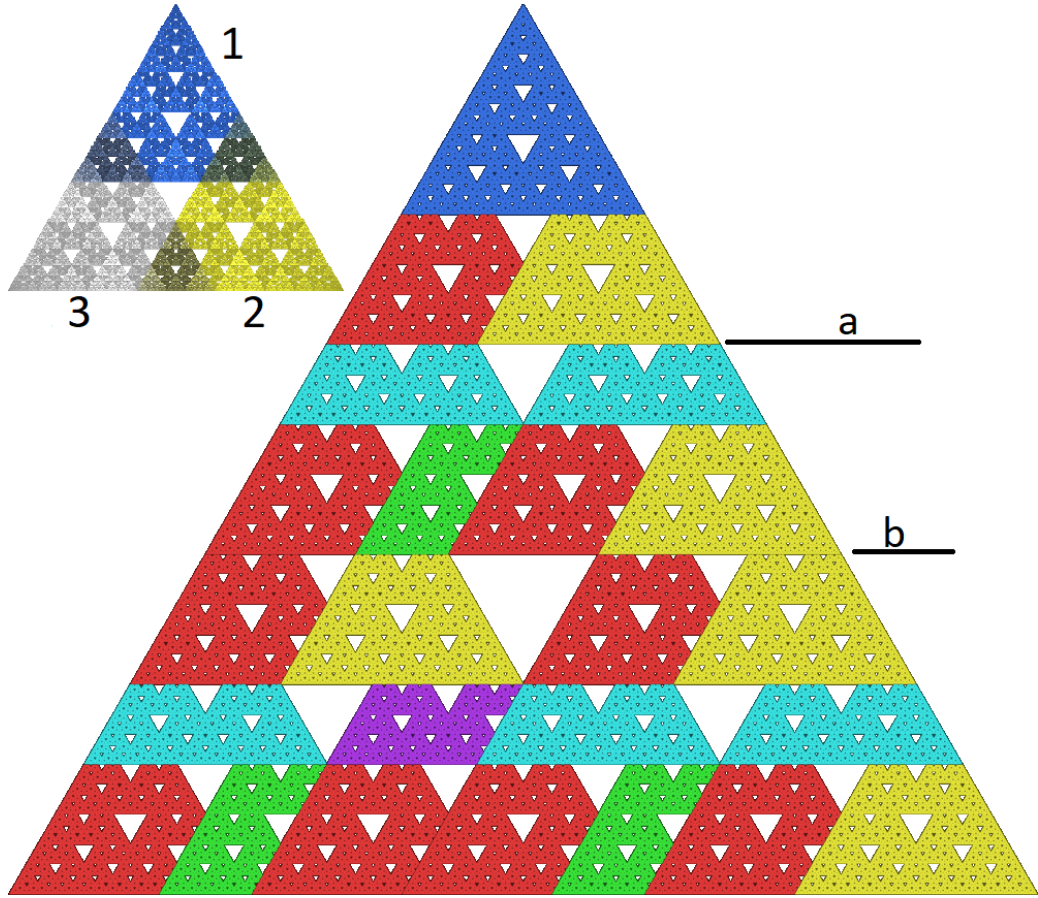


Figure 2: The golden triangle with overlaps, and as a non-overlapping GIFS on level 3.

We now explain the GIFS. The construction is derived in the next section. Colors and notation of Figure 2 follow the first example. The uppermost three triangles above line a illustrate the equation

$$B_1 = f_1(B_1) \cup f_2(B_2) \cup f_3(B_3),$$

where the yellow set B_2 is pruned at the upper part and the red set B_3 at the upper and right parts. The second level subdivision is above line b . Between lines a and b it can be seen how B_2 and B_3 are subdivided with the help of new sets B_4, B_5 drawn in turquoise and green, respectively:

$$B_2 = f_1(B_4) \cup f_2(B_2) \cup f_3(B_3), \quad B_3 = f_1(B_4) \cup f_2(B_5) \cup f_3(B_3).$$

In the third level we see how B_4 and B_5 are decomposed. For B_5 we need the purple set B_6 . The subdivision of B_6 would show up on level 4. Here it can be seen at the triangle's left corner.

$$B_4 = f_2(B_2) \cup f_3(B_3), \quad B_5 = f_1(B_6) \cup f_3(B_3), \quad B_6 = f_2(B_5) \cup f_3(B_3)$$

These sets have only two pieces since a whole triangle piece was cut off. The system of six set equations together with the IFS (7) determine the GIFS which clearly fulfils the open set condition (4). The open sets $U_k, k = 1, \dots, 6$ can be taken as interiors of the convex hulls of the respective sets B_k .

To calculate the dimension, consider the 0-1-matrix $M = (m_{k\ell})$ with $m_{k\ell} = 1$ if B_ℓ appears on the right side of the equation for B_k . All attractors B_k have the same dimension β since M is irreducible [40]. The characteristic polynomial of M is $p(\lambda) = \lambda(\lambda - 1)(\lambda + 1)(\lambda^3 - 3\lambda^2 + 3)$, with spectral radius $\lambda_{\max} \approx 2.532$. So $\beta = \log \lambda_{\max} / -\log t \approx 1.9306$. The trick with $\mu(f_i(A)) = t^\beta = s$ in the example above gives $1 = 3s - 3s^3$ since $f_i(A) \cap f_j(A)$ is a piece of level 3. This implies $s = 1/\lambda_{\max}$. In [18], an infinite IFS leads to the polynomial, and it is mentioned that $s = (2/\sqrt{3}) \cos(7\pi/18)$.

3 The overlap graph

Let an IFS $F = \{f_1, f_2, \dots, f_m\}$ with overlapping attractor A be given. The numbering of the maps can be chosen arbitrarily. It will be important since for overlapping pieces $f_i(A), f_j(A)$, we shall cut away the intersection from the piece with larger index in the lexicographic order.

Around 2000, a data structure was developed which controls the intersections of pieces $f(A) \cap g(A)$ with $f, g \in F^*$ [1, 5, 23, 34, 36, 43, 46, 49]. For many examples, the standardized intersections $f^{-1}g(A) \cap A$, the outer boundary sets, form a graph IFS. Moreover, it is easier to calculate with mappings $f^{-1}g$ than with boundary sets. This led to the neighbor graph which has vertices $h = f^{-1}g$ with $f, g \in F^k$ for some $k \in \mathbb{N}$ for which $f(A) \cap g(A) \neq \emptyset$. Such maps h are called proper neighbor maps. Each of these maps represents the relative position of two intersecting pieces of A , up to similarity. Since pieces in different levels have different size, the map f^{-1} performs a standardization, so that the first piece becomes A and the second $h(A)$.

If there exist only finitely many proper neighbor maps, the IFS is said to be of finite type. The neighbor maps can be defined recursively, starting with the identity map id and repeatedly applying the formula $h' = f_i^{-1}h f_j$ for all $i, j \in \{1, \dots, m\}$. Whenever this relation holds, we draw an edge with label (i, j) from vertex h to vertex h' . If the IFS is of finite type, the recursive procedure will be completed after finitely many steps. For this construction, we refer to [6, 7, 10, 11] and recent related work [29, 38, 39, 46, 52]. This paper takes the neighbor graph as given and discusses its application.

We do not need the full neighbor graph. We are only interested in intersections $f(A) \cap g(A)$ which contain complete overlaps. That is, there exist $f', g' \in F^*$ such that $ff'(A) = gg'(A)$. In this case $f'^{-1}f^{-1}gg' = id$ which implies that in the neighbor graph there is a path of edges from $h = f^{-1}g$ to id . Thus we consider the subgraph of the neighbor graph determined by all vertices h which admit a directed path to id . This graph will be called the *overlap graph*.

Proposition 1 *The overlap graph is obtained from the neighbor graph by matrix operations.*

Proof. Let M be the $n \times n$ adjacency matrix of the neighbor graph: $m_{k\ell} = 1$ if there is an edge from vertex k to ℓ , and zero otherwise. Let the initial vertex id correspond to $k = 1$. Determine the matrix $N = M + M^2 + \dots + M^{n-1}$. Note that $n_{k\ell}$ is the number of directed paths of length $\leq n - 1$ from vertex k to vertex ℓ . The adjacency matrix O of the overlap graph is

the submatrix of M given by the rows of N with non-zero first entry, and the corresponding columns. The labels of edges remain unchanged.

For large n , we avoid overflow and reduce the number of matrix multiplications from n to $2 \log_2 n$ as follows. Start with $B = N = M$ and let k be the integer part of $\log_2 n$. Then repeat k times $N = \min(B * N + N, 1)$; $B = \min(B * B, 1)$ where the minimum is taken in every cell of the matrix. \square

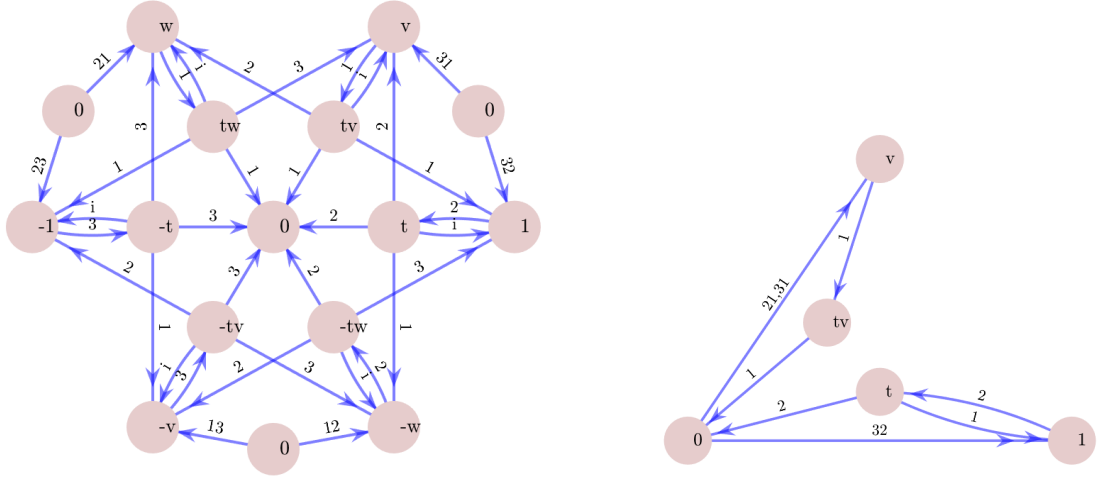


Figure 3: The overlap graph for the golden triangle. To minimize intersections of edges, the initial vertex 0 was drawn three times, and once as terminal vertex in the middle. For the construction of the GIFS, it is sufficient to consider the small subgraph on the right.

Before we go to details, we briefly review the structure of the overlap graph. Each vertex represents a standardized overlap set $A \cap h(A)$ and the corresponding neighbor map h . There is one initial vertex id or 0 , which represents the complete overlap $A = h(A)$. From the initial vertex arise edges with label (i, j) for all $i, j \in \{1, \dots, m\}$ for which $f_i(A)$ and $f_j(A)$ overlap. For another vertex which represents h and the overlap $D = A \cap h(A)$, there arise edges with label i for the i with nonempty overlap $D_i = f_i(A) \cap D$. The terminal vertex of such an edge is the standardized overlap of the i -th piece, $E_i = f_i^{-1}(D_i)$ which is larger than D_i , and $D = \bigcup_i f_i(E_i)$.

The overlap graph of the golden triangle is shown in Figure 3. The full neighbor graph has 18 more vertices describing intersections of neighboring pieces in a single point. For the IFS (7), all neighbor maps are translations. So vertices are denoted by translation vectors. There are translations by the sixth roots of unity, called $\pm 1, \pm v, \pm w$ with $w = v - 1$, which correspond to overlaps in a small triangle. Translations by the smaller vectors $\pm t, \pm tv, \pm tw$ with $t = \frac{1}{2}(\sqrt{5} - 1)$ correspond to large triangular overlaps. It will be sufficient to label edges with a single number i instead of (i, j) . Only for the edges starting in $id = 0$ we kept the full notation. The letter i itself means “1 or 2 or 3”. The vertex $id = 0$ was drawn at four places in order to avoid more intersections of edges.

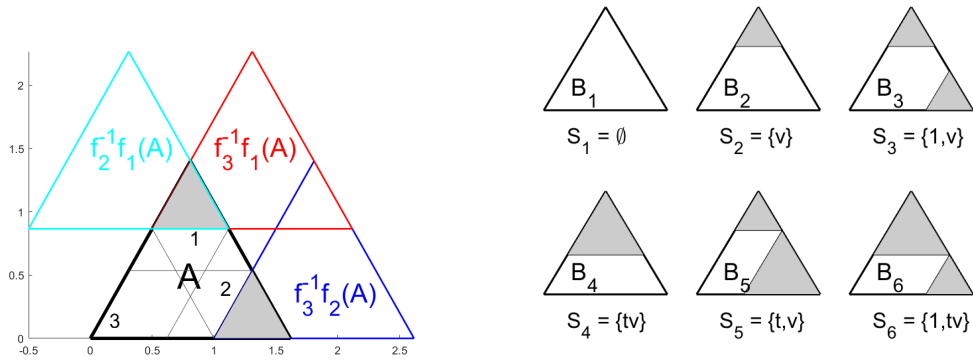


Figure 4: Left: The initial overlaps for the golden triangle. Right: The six attractors B_k . Cut overlaps are shaded.

Figure 4 illustrates the neighbor maps $h = f_i^{-1}f_j$ which correspond to edges starting at the initial vertex 0. We assume $i > j$ since only in this case the neighbor has a lexicographically smaller address and the piece under consideration must be reduced. The side length of the triangle A is $t + 1 = 1/t \approx 1.618$, as indicated in Figure 4. From (7) immediately follows $f_3^{-1}f_2(z) = z + 1$ and $f_3^{-1}f_1(z) = z + v$. In Figure 3 this gives the two edges labelled 32 and 31 from 0 on the upper right to the vertices 1 and v . The translation vectors 1 and v represent the two shaded overlap triangles which every piece of type 3 must have with its immediate neighbors. They must be cut away since the neighbors have smaller address. We called the piece B_3 , and now we associate it with the overlap set $S_3 = \{1, v\}$ while the set $B_1 = A$ has no overlap so that $S_1 = \emptyset$. For the piece B_2 we cut away only the upper small triangle which corresponds to the overlap set $S_2 = \{w\}$ since $f_2^{-1}f_1(z) = z + w$.

Because of symmetry, v and w describe the same overlap set. When we put them together, we can use the small subgraph in Figure 3 for the following discussion. We interpret 1 and v as ‘small overlaps at the right and the top’, shaded in Figure 4, and t, tv as ‘large overlaps at the right and the top’, respectively.

The attractors B_1, B_2 , and B_3 were obtained from initial edges of the overlap graph. The corresponding sets S_k contain the terminal vertices of these edges. Each vertex represents a neighbor map h , in our case a translation by 1, v , or w , which is applied to cut away an overlap. Formally

$$B_k = \text{cl}\left\{A \setminus \bigcup_{h \in S_k} h(A)\right\},$$

where cl denotes topological closure. This is the basic formula for all B_k . Non-initial edges determine the overlaps of subpieces from the overlap of a piece. As an example, we establish the equation for B_3 with $S_3 = \{1, v\}$. For piece 1 of B_3 , we study edges with label 1 and initial vertex in S_3 . There is only one: from v to vertex tv . The small overlap v at the top of B_3 becomes a large overlap tv of its piece 1. Thus piece 1 of B_3 is determined by the new vertex set $S_4 = \{tv\}$, corresponding to B_4 in Figure 4 and to the turquoise set in Figure 2.

For piece 2 of B_3 we consider edges with label 2 from S_3 . The only edge from 1 to t indicates that the small overlap at the right of B_3 becomes a large overlap of the piece 2. Moreover, piece 2 has the overlap $v = w$ at the top, since it must respect piece 1 inside B_3 . Thus piece 2 has the new vertex set $S_5 = \{t, v\}$ corresponding to the green set B_5 in Figure 2. Since there are no edges with label 3 from S_3 , piece 3 of B_3 has only the overlaps $S_3 = \{1, v\}$ imposed by pieces 1 and 2. So piece 3 corresponds to B_3 . The resulting equation is $B_3 = f_1(B_4) \cup f_2(B_5) \cup f_3(B_3)$.

Now consider B_4 with $S_4 = \{tv\}$. There is an edge labelled 1 from tv to 0. This means that piece 1 of B_4 does not exist - it is contained in the overlap which was cut off. Piece 2 of B_4 has only the overlap $S_2 = \{v\}$ (caused not by piece 1, but by the cutoff). Piece 3 again corresponds to S_3 . The equation is $B_4 = f_2(B_2) \cup f_3(B_3)$. For B_5 with $S_5 = \{t, v\}$ piece 2 disappears, and piece 1 has overlaps $S_6 = \{1, tv\}$ corresponding to another attractor B_6 . Overlap 1 at the right of piece 1 is caused by cutting off piece 2. In this way we find the system of equations directly from the overlap graph.

4 Cut overlaps and neighborhoods

Our approach is quite similar to the work of Ngai and Wang [43] which bases on the idea of neighborhood graph developed by Lalley [34]. In both cases, the number of different overlaps must be finite, up to similarity. The overlapping attractor A is replaced by modifications which we may call types. In our case the types B_k are copies of A with cut overlaps, as can be seen in Figure 4. In [34, 43] neighborhood types A_k are considered. These are pieces of A with a certain environment inside A , that is, neighbors overlapping them in a specific way. In both approaches, types are determined by sets of overlaps. For the golden triangle, a piece can have two, three, four, or six neighbors. In the case of four neighbors, three different configurations are possible. Figure 5 shows the resulting types numbered 1 to 6. Type 0, a set without neighbors which would correspond to our B_1 , was omitted.

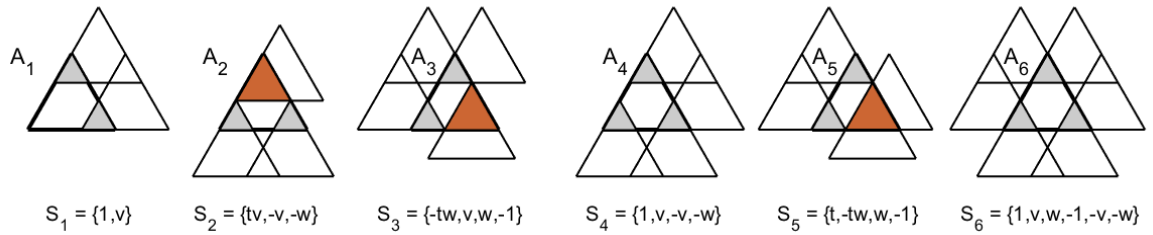


Figure 5: The six nontrivial neighborhood types of pieces in the golden triangle. Reflected and rotated neighborhoods have the same type. The brown pieces represent complete overlaps and cause rational entries in the substitution matrix.

Rotated and reflected neighborhood types are considered to be identical. Otherwise we would have 21 types for the golden triangle. Using symmetry, the number of types is reduced. As a consequence, a type is given by a whole symmetry class of overlap sets. S_k in Figure 5 is only

one representative. In contrast, our approach is symmetry-breaking. The sets B_k do not show much symmetry. Their type is given by their very shape which makes our approach simple.

For each type A_k or B_k , the types of the pieces $f_i(A_k)$ or $f_i(B_k)$ are determined for $i = 1, \dots, m$ in both approaches. In this way, Lalley, Ngai and Wang obtain a neighborhood graph while we obtain a system of GIFS equations. In both cases, this results in a “substitution matrix”. The Hausdorff dimension of A is $\beta = \log \sigma / -\log r$ where σ denotes the spectral radius of the substitution matrix. The GIFS structure is more powerful since it determines various other topological and measure-theoretical properties of A . One can ask whether the neighborhood approach also leads to a GIFS structure.

$$\begin{pmatrix} 1 & 1 & 0 & 0 & 0 & 0 \\ 0 & 1 & 1 & 1/2 & 0 & 0 \\ 0 & 0 & 1 & 1/2 & 1 & 0 \\ 0 & 2 & 0 & 0 & 1 & 0 \\ 0 & 0 & 2 & 0 & 0 & 1/3 \\ 0 & 0 & 0 & 0 & 3 & 0 \end{pmatrix}$$

Table 1: The rational “substitution matrix” for the neighborhood types $i = 1, \dots, 6$ of the golden triangle. Row i counts the successors of a specimen of type i according to successor type.

In general, this is not the case. The problem is that a substitution matrix with integer entries need not exist, not even for the golden triangle. Apparently, this has gone unnoticed until now. The problem comes with the neighborhoods of pieces which represent complete overlaps, shaded brown in Figure 5. This piece in A_2 is a successor of type A_4 . And it is also a successor A_4 of the upper neighbor of the parent. Each A_4 piece either has two A_2 parents, or two A_3 parents, and no other predecessors. Thus each A_2 or A_3 piece has 1/2 successor of type A_4 .

It is possible to circumvent the problem by counting A_2 and A_3 together, as has been done for other examples in [43]. However, type A_6 with six neighbors is the child of three different parents A_5 and has no other predecessors. There is nothing to count together. The number of type A_6 successors of A_5 must be 1/3 since three specimen of A_5 share one successor A_6 . We do not go into details and present only the rational substitution matrix. Its characteristic polynomial is identical to the polynomial $p(\lambda)$ of our substitution matrix at the end of Section 2. Apparently, the Hausdorff dimension calculation in [43] remains true when the substitution matrix contains rational entries. Further structural information seems out of reach with the neighborhood approach, however.

5 Combinatorial construction of the GIFS

Now we derive the GIFS equations in the general case. The method, based on calculations with graphs and matrices instead of overlaps and geometry, can be implemented on a computer. In \mathbb{R}^d , we are given an IFS $F = \{f_1, f_2, \dots, f_m\}$ of similitudes with equal contraction factor and

with overlapping attractor

$$A = \bigcup_{j=1}^m f_j(A). \quad (8)$$

The indexing of the maps can be chosen arbitrarily but must be fixed for the construction. We assume that the overlap graph with vertex set S is given. It can be determined from the neighbor graph by Proposition 1. The construction of the neighbor graph is known [6, 7, 10, 11, 29, 38, 39, 46, 52].

Side remark. The overlap graph could be directly constructed from inverse iteration starting in id . Thus we really need only the finite overlap type condition and not the finite type condition which is formally stronger and needed for the neighbor graph. All known examples with overlaps and finite overlap type are finite type. See [6, Section 2] for a discussion of these subtleties.

Step by step, the equation for A is replaced by a system of equations (3) for the attractors B_1, \dots, B_n . Each B_k is represented by a set of vertices $S_k \subseteq S$. All calculations are done with the S_k . The algorithm is based on (10) and (12) below. Nevertheless, we add the interpretation for the sets B_k so that the operations for the S_k can be understood. We choose the S_k so that the

$$B_k = \text{cl}\{A \setminus \bigcup_{h \in S_k} h(A)\}, \quad (9)$$

with cl denoting topological closure, fulfil the GIFS equations in a non-overlapping way. The algorithm consists of an initialization and a recursion. The number of equations is not known at the beginning. The edges of the overlap graph starting in id are labelled (i, j) . For all other edges only the first label i is needed. We use $t \xrightarrow{i} s$ as shorthand for “there is an edge from t to s with label i ”.

Initialization. Let $S_1 = \emptyset$. For $i = 2, \dots, m$ let

$$S_i = \{s \in S \mid id \xrightarrow{(i,j)} s \text{ for some } j < i\}. \quad (10)$$

According to (9), this implies $B_1 = A$ and $B_i = \text{cl}\{A \setminus \bigcup_{j < i} f_i^{-1} f_j(A)\}$. Thus $f_i(B_i)$ is the closure of $f_i(A) \setminus \bigcup_{j < i} f_j(A)$. In the case that $B_i = \emptyset$ we remove f_i from the IFS without changing A and start the construction with the reduced IFS. By (8), the first equation

$$B_1 = \bigcup_{i=1}^m f_i(B_i)$$

is now fulfilled, and the overlaps have been removed. Put $k = 1$ and $n = m$. At the end of the initialization, we remove double names for $i = 2, \dots, m$. When S_i coincides with S_j for some $j < i$, we use the names S_j and B_j for S_i and B_i . Then we reduce the index of all S_k, B_k with $i < k \leq n$ by one and replace n by $n - 1$. Now and in the future n and k denote the current number of different attractors and of established equations, respectively.

Recursion. Let $k = k + 1$, which means we establish a new equation. It has the form

$$B_k = \bigcup_{i=1}^m f_i(B_{ik}). \quad (11)$$

To this end, we define for $i = 1, \dots, m$ the sets

$$S_{ik} = S_i \cup \{s \in S \mid t \xrightarrow{i} s \text{ with } t \in S_k\} \text{ with } S_i \text{ from (10)}. \quad (12)$$

According to (9), the set B_{ik} is obtained by subtracting from A the overlaps corresponding to the vertices of S_{ik} . The subset $S_i \subseteq S_{ik}$ cares for the internal overlaps of the pieces of B_k , as in the initialization. The second part of S_{ik} guarantees that $f_i(B_{ik}) \subseteq B_k$. The overlaps t of the big set B_k are expressed as overlaps of its pieces. If there is no edge $t \xrightarrow{i} s$ then the overlap t does not hit piece i . If there is such an edge, however, the overlap s has to be subtracted from B_{ik} . In this way, (12) enforces the validity of the equation for B_k . For certain i , the overlaps can cover the set A . This always happens if $id \in S_{ik}$. In that case (9) says $B_{ik} = \emptyset$.

After each recursion step, the terms with $B_{ik} = \emptyset$ are omitted from the equation and the other S_{ik} are renamed for $i = 1, \dots, m$. If $S_{ik} = S_\ell$ for some $\ell \leq n$, we use the names S_ℓ and B_ℓ to avoid duplicates. Otherwise, we set $n = n + 1$ and introduce the new name S_n for S_{ik} . This means that later we have to build another equation for B_n . The renumbering step transforms the equation (11) into the form (3). The recursion has to be repeated until $k = n$. Then each $B_\ell, \ell = 1, \dots, n$ is expressed by a GIFS equation.

Proposition 2 (i) *The recursion procedure finishes after finitely many steps.*

(ii) *For an IFS with the given overlap graph, the constructed system of equations (11) has the unique solution given by (9), $k = 1, \dots, n$. In particular $B_1 = A$.*

Proof. (i). The finite set S has only finitely many subsets which can appear as S_k . In a related context, this argument was mentioned already 1989 by Thurston [51, Section 9]. The theoretical bound $n \leq 2^{\text{card } S}$ is huge. Our experimental work will show that in practice the number of equations is much smaller. (ii). For an IFS with contractive maps, any GIFS system of equations (3) has a unique solution consisting of compact nonempty sets B_k [40]. Since the S_k were constructed so that the B_k with (9) fulfil the equations, this must be the solution. \square

6 Proof of the open set condition

We now prove Theorem 1. The GIFS equations (3) and the family of compact non-empty attractors B_1, \dots, B_n were constructed above. We must define the open sets U_1, \dots, U_n and show that they fulfil (4). The proof for attractors with non-empty interior will serve as a blueprint for the general case.

Proof for $\text{int } A \neq \emptyset$. In this case the definition is simple: $U_k = \text{int } B_k$. Thus $U_1 = \text{int } A \neq \emptyset$. At the initialization of the algorithm, before renumbering,

$$U_k = \text{int } A \setminus \bigcup_{j=1}^{k-1} f_k^{-1} f_j(A) \text{ for } k = 2, \dots, m$$

which implies that the $f_k(U_k) = f_k(\text{int } A) \setminus \bigcup_{j=1}^{k-1} f_j(A) \subset U_1 \setminus \bigcup_{j=1}^{k-1} f_j(U_1)$ are disjoint subsets of U_1 . Moreover $U_k \neq \emptyset$ since we assumed $B_k \neq \emptyset$. So the OSC is fulfilled for $k = 1$.

Any self-similar set A with non-empty interior is regular-closed. That is, $\text{cl}(\text{int } A) = A$. The definition (9) of B_k can be reformulated as $B_k = \text{cl}\{\text{int } A \setminus \bigcup_{h \in S_k} h(A)\}$ because the finite union is compact. Thus all B_k and B_{ik} are regular-closed. In an equation (11) for $k > 1$, the set $U_{ik} = \text{int } B_{ik}$ can only be empty if B_{ik} is empty. As above, the first part of the definition (12) implies that the sets $f_i(U_{ik}), i = 1, \dots, m$ are disjoint. The second part of (12) together with (9) guarantees that $f_i(B_{ik}) \subset B_k$ and consequently $f_i(U_{ik}) \subset U_k$. This proves the OSC for the equations (11). Renaming the B_{ik}, U_{ik} brings them to the form (3) and preserves the OSC. \square

Proof of the general case. We work with neighbor maps $h = f^{-1}g$ where $f, g \in F^*$. Let N denote the infinite set of all such neighbor maps for which $h(A)$ does not contain a whole piece of A . In particular, the (infinite) neighbor graph must not contain a (finite) directed path of edges from h to id . Our open sets should not intersect these non-overlapping neighbors. We use central open sets [9, 13] and define

$$\begin{aligned} U_1 &= \{x \in \mathbb{R}^d \mid d(x, A) < \inf_{h \in N} d(x, h(A)) = d(x, \bigcup_{h \in N} h(A))\} , \\ U_k &= \{x \in \mathbb{R}^d \mid d(x, B_k) < \inf_{h \in N \cup S_k} d(x, h(A))\} \text{ for } k = 1, \dots, n, \end{aligned} \quad (13)$$

and similar for the U_{ik} with U_k, B_k, S_k replaced by U_{ik}, B_{ik}, S_{ik} , respectively. Here $d(x, A) = \inf\{|x - y| : y \in A\}$ denotes the distance from a set. Proposition 3 below shows that U_1 contains a dense subset of A . Since $B_k \subset A$, this implies that U_k can only be empty if $B_k \subseteq \bigcup_{h \in S_k} h(A)$. That would mean $B_k = \emptyset$. This argument also shows $U_{ik} \neq \emptyset$ unless $B_{ik} = \emptyset$.

For the initialization step we have to show that the $f_k(U_k)$ with $k = 1, \dots, m$ are subsets of U_1 , and that they are disjoint. First we note that $U_k \subseteq U_1$ because $B_k \subseteq A$ and so for $x \in U_k$

$$d(x, A) \leq d(x, B_k) < \inf_{h \in N \cup S_k} d(x, h(A)) \leq \inf_{h \in N} d(x, h(A)) .$$

Thus it suffices to show that the $f_k(U_1)$ are subsets of U_1 . Let $K = \bigcup_{h \in N} h(A)$. Take a point $x \in U_1$ and its image $y = f_k(x)$. Since f_k is a similitude with factor r ,

$$d(y, A) \leq d(y, f_k(A)) = rd(x, A) < rd(x, K) = d(y, f_k(K)) \leq d(y, K) .$$

We used $K \subseteq f_k(K)$ which follows from the fact that each $h(a)$ with $a \in A$ and $h \in N$ can be written as $f_k(f_k^{-1}hf_j(a'))$ for at least one j for which $a \in f_j(A)$ and $a' = f_j^{-1}(a)$. The neighbor map $h' = f_k^{-1}hf_j$ is a successor of h in the neighbor graph. So it belongs to N whenever h does. We have proved $f_k(U_1) \subseteq U_1$.

Next we show that $f_j(U_j) \cap f_i(U_i) = \emptyset$ for $1 \leq j < i \leq m$. Due to the definition $B_i = \text{cl}\{A \setminus \bigcup_{h \in S_i} h(A)\}$ the sets B_j, B_i are closed subsets of A , and the intersection $f_j(B_j) \cap f_i(B_i)$ is relatively small: when $f_j(A) \cap f_i(A)$ is an overlap, then $f_i^{-1}f_j$ is in S_k , and $f_i^{-1}f_j(A)$ is subtracted before taking the closure to obtain B_i . For $x \in U_i$ the definition states $d(x, B_i) < d(x, f_i^{-1}f_j(A))$. Applying f_i on both sides we get

$$d(f_i(x), f_i(B_i)) < d(f_i(x), f_j(A)) \leq d(f_i(x), f_j(B_j)) .$$

Thus the points of $f_i(U_i)$ are closer to $f_i(B_i)$ than to $f_j(B_j)$.

On the other hand, for an arbitrary small piece $g(A)$ with $g \in F^*$ which does not intersect $f_j(A)$, the neighbor map $h = f_j^{-1}g$ belongs to N since $A \cap h(A) = \emptyset$. There is a countable family $G \subset F^*$ such that the pieces $g(A)$ do not meet $f_j(A)$ and cover a dense subset of $f_i(B_i)$. According to the definition (13) we have for $x \in U_j$

$$d(x, B_j) < \inf_{h \in N \cup S_j} d(x, h(A)) \leq \inf_{g \in G} d(x, f_j^{-1}g(A)) = d(x, f_j^{-1}(\bigcup_{g \in G} g(A))) \leq d(x, f_j^{-1}f_i(B_i)).$$

Applying f_j on both sides, we see that the points of $f_j(U_j)$ have smaller distance to $f_j(B_j)$ than to $f_i(B_i)$. Together, the two statements imply that $f_j(U_j)$ and $f_i(U_i)$ are disjoint. The OSC for the first equation of the GIFS is verified.

For the equations $B_k = \bigcup_{i=1}^m f_i(B_{ik}), k = 2, \dots, n$ the definition (13) and the proof of the disjointness of the $f_j(U_{jk})$ are the same, only with B_i, U_i, S_i replaced by B_{ik}, U_{ik}, S_{ik} . The challenge is to prove $f_i(U_{ik}) \subseteq U_k$ for $i = 1, \dots, m$. Consider a point $y \in U_{ik}$ and its image $x = f_i(y) \in f_i(U_{ik})$. We show condition (13) for x . The definition (12) of S_{ik} guarantees $f_i(B_{ik}) \subseteq B_k$. Thus

$$d(x, B_k) \leq d(x, f_i(B_{ik})) = rd(y, B_{ik}) < r \inf_{h \in N \cup S_{ik}} d(y, h(A)) = C$$

according to definition (13) of U_{ik} . Now C is the minimum of two terms:

$$r \inf_{h \in N} d(y, h(A)) = \inf_{h \in N} d(x, f_i h(A)) \leq \inf_{h \in N} d(x, h(A))$$

because of $f_i(K) \subseteq K$ as shown above, and

$$r \inf_{h \in S_{ik}} d(y, h(A)) \leq r \inf_{h \in S_{ik}^*} d(y, h(A)) = r \inf_{h \in S_k} d(y, f_i h(A)) \leq \inf_{h \in S_k} d(x, h(A)).$$

Here $S_{ik}^* = \{s \in S \mid t \xrightarrow{i} s \text{ with } t \in S_k\}$ is the second part of S_{ik} in (12) which by definition of the neighbor graph refers to the overlaps $f_i^{-1}h(A)$ with $h \in S_k$. Taking the minimum of the two upper bounds we obtain

$$d(x, B_k) < C \leq \inf_{h \in N \cup S_k} d(x, h(A))$$

which says that x belongs to U_k by (13).

Last not least we prove that U_1 is nonempty. Fix some $\varepsilon > 0$ and let $A^\varepsilon = \{x \mid d(x, A) < \varepsilon\}$. For $\ell = 1, 2, \dots$ and $f \in F^\ell$ let

$$\gamma(f) = \text{card}\{g \in F^\ell \mid g(A) \cap f(A^\varepsilon) \neq \emptyset\}$$

denote the number of pieces of the same size near $f(A)$. Note that equal mappings, as well as overlaps, must be counted only once. Now set $\gamma = \sup_{f \in F^*} \gamma(f)$. Zerner proved that, independently of ε , the IFS F fulfils the WSC if and only if $\gamma < \infty$ [54], [12, Section 4.2]. For Theorem 1 we assumed that F fulfils the WSC. So γ is a positive integer, hence $\gamma = \gamma(\bar{f})$ for some $\bar{f} \in F^*$. Define the open set

$$V = \bigcup_{g \in F^*} g\bar{f}(A^\varepsilon).$$

This set was introduced by Schief [47] in the OSC setting [12, Section 4.1]. Obviously V contains a dense subset of A .

Proposition 3 $V \cap h(A) = \emptyset$ for $h \in N$, and $V \cap A \subset U_1$.

Proof. Let $h = \tilde{f}^{-1}\tilde{g}$ with $\tilde{f}, \tilde{g} \in F^*$. We assume that there is a point

$$x \in h(A) \cap V = \tilde{f}^{-1}\tilde{g}(A) \cap \bigcup_{g \in F^*} g\bar{f}(A^\varepsilon)$$

and show that h is not in N . We fix a $g \in F^*$ such that $\tilde{f}(x) \in \tilde{g}(A) \cap \tilde{f}g\bar{f}(A^\varepsilon)$. Suppose that $\bar{f} \in F^\ell$. The definition of $\gamma = \gamma(\bar{f})$ says that there exist mappings $g_j \in F^\ell$ with $g_j(A) \cap \bar{f}(A^\varepsilon) \neq \emptyset$ for $j = 1, \dots, \gamma$. Thus there are $\gamma + 1$ pieces $\tilde{g}(A)$ and $\tilde{f}gg_j(A)$ which all intersect $\tilde{f}g\bar{f}(A^\varepsilon)$.

To obtain a contradiction to the maximality of γ , we need pieces of equal size. Let $\tilde{f}gg_j$ have length L , and $\tilde{g} = f_1f_2 \cdots f_k$ with $f_i \in F$. We replace \tilde{g} by \bar{g} with length L . If $k \geq L$, we define $\bar{g} = f_1f_2 \cdots f_L$ for which $\bar{g}(A) \supseteq \tilde{g}(A)$. If $k < L$, we select further maps $f_{k+1}, \dots, f_L \in F$ such that $\bar{g}(A)$ with $\bar{g} = f_1f_2 \cdots f_L$ contains $\tilde{f}(x)$.

The contradiction to the maximality of γ implies that $\bar{g} = \tilde{f}gg_j$ for some j between 1 and γ . Then $\tilde{f}^{-1}\bar{g} = gg_j$ represents a complete overlap which implies that $h = \tilde{f}^{-1}\tilde{g}$ is not in N . This proves the first assertion of the proposition.

The second assertion is a direct consequence. For $x \in V$, we have $d(x, \bigcup_{h \in N} h(A)) \geq d(x, \mathbb{R}^d \setminus V) > 0$. Thus any $x \in V \cap A$ belongs to U_1 by definition (13). \square

Theorem 1 is proved. The rest of the paper is devoted to concrete examples.

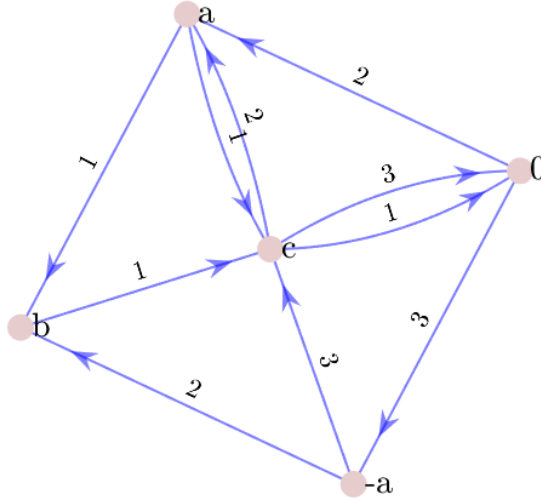


Figure 6: A small overlap graph for which we determine the non-overlapping GIFS.

7 A small example

The GIFS will be constructed for the overlap graph of Figure 6 without knowledge of the IFS and the geometry of the attractor. We have three maps f_1, f_2, f_3 . There are only two edges

starting in the initial state 0, with first labels 2 and 3. Second labels must then be 3 and 2, respectively. Thus only $f_2(A)$ and $f_3(A)$ overlap, and we must subtract the overlap from piece 3 which is lexicographically larger. Thus our first equation is

$$B_1 = f_1(B_1) \cup f_2(B_1) \cup f_3(B_2)$$

where B_2 is characterized by $S_2 = \{-a\}$, the endpoint of the initial edge with label 3. For the equation of B_2 , we have to consider the successors of S_2 in Figure 6 with label 1,2, and 3, and only for label 3 we have to add $S_2 = \{-a\}$. There is no edge with label 1, an edge with label 2 to b and an edge with label 3 to e . According to (12) we have $S_{12} = \emptyset = S_1, S_{22} = \{b\} = S_3$ and $S_{32} = \{e, -a\} = S_4$, leading to the equation

$$B_2 = f_1(B_1) \cup f_2(B_3) \cup f_3(B_4) .$$

From $S_3 = \{b\}$ there is only one edge with label 1 to vertex e , so $B_3 = f_1(B_5) \cup f_2(B_1) \cup f_3(B_2)$ with $S_5 = \{e\}$. Now consider $S_4 = \{e, -a\}$. From e there are edges with labels 1 and 3 to the initial vertex 0. That means that the first and third part of B_4 disappear, and only the term with label 2 remains in the equation:

$$B_4 = f_2(B_6) \text{ with } S_6 = \{b, a\}. \quad \text{Similarly, } B_5 = f_2(B_7) \text{ with } S_7 = \{a\}.$$

Using the successors of S_6 and S_7 , we obtain the equations

$$B_6 = f_1(B_8) \cup f_2(B_1) \cup f_3(B_2) \quad \text{and} \quad B_7 = f_1(B_8) \cup f_2(B_1) \cup f_3(B_2)$$

with $S_8 = \{b, e\}$, and, finally, $B_8 = f_2(B_7)$.

Since the equations determine their attractors, we have $B_6 = B_7$ and $B_8 = B_5$, which then imply $B_5 = B_4$ and $B_7 = B_3$. The simplified GIFS system with four attractors consists of the equations for B_1 and B_2 and

$$B_3 = f_1(B_4) \cup f_2(B_1) \cup f_3(B_2) , \quad B_4 = f_2(B_3) .$$

Figure 7 shows the overlapping attractor A and the non-overlapping GIFS attractor B_1 on levels 1,2, and 3. The coloring of the pieces illustrates the equations for B_1, \dots, B_4 . This example, based on a complex Pisot number of order 4, was introduced and discussed in [6, Figure 5 and Section 4.2].

One can ask why we got a redundant system. The reason is an ambiguity of our coding of overlaps. Each set S_k characterizes a corresponding overlap set $D_k = \bigcup_{s \in S_k} A \cap s(A)$ where the vertices s of the overlap graph are also neighbor maps. An inclusion $S_k \subseteq S_\ell$ implies $D_k \subseteq D_\ell$. However, overlap sets D_k can also be subsets of each other, or even coincide, when the corresponding sets of vertices S_k are not at all related.

In the present example, the overlap $D_e = A \cap e(A)$ is very large, containing the first and third piece of A and a part of the second one. It contains the overlaps D_b, D_a , and D_{-a} . Moreover, $D_a = D_b$. If we knew this, we would have identified S_4 with S_5 , and S_6 with S_3 , and would have obtained the simple system of four equations immediately.

Actually, we can determine the overlaps D_s for all vertices s mathematically, without further knowledge of the IFS. The addresses of the points in D_s are given by the sequences of labels

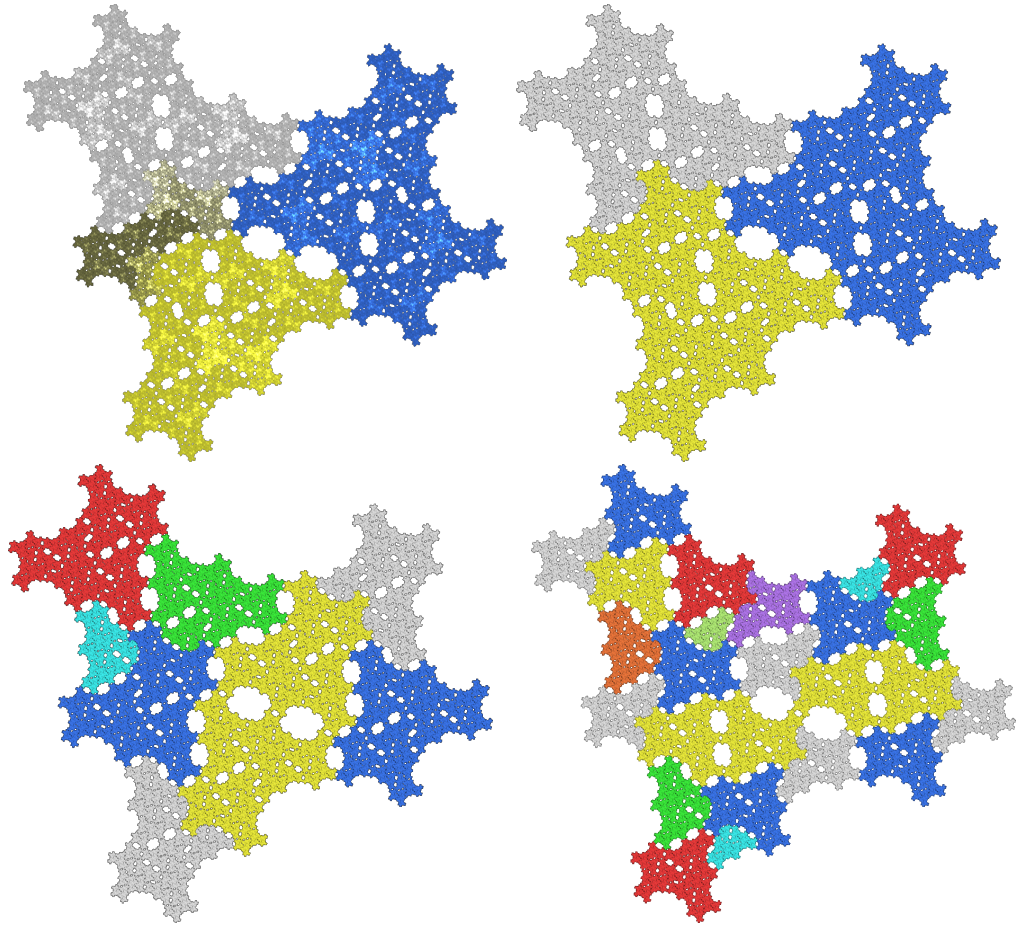


Figure 7: Top: A WSC attractor A with cloudy overlaps, introduced in [6], and the GIFS attractor B_1 with clear structure. Bottom: B_1 on level 2 and 3. Pieces of type B_1 are blue, yellow, and red, B_2 gray and pink, B_3 green and brown, B_4 turquoise and light green.

of directed edge paths starting in vertex s [7], using the convention that there are loops from 0 to 0 with label i for $i = 1, \dots, m$. Instead of infinite edge paths, we can also consider finite edge paths from s to 0, which describe the interior of D_s as a countable union of overlap pieces. This is standard in automata theory, s is the initial and 0 the final state, and the words labelling the edge paths from s to 0 form a regular language L_s [31, 24]. For $s = e$ we have $L_e = (21)^* \{1, 3\}$ which denotes the union of pieces 1, 3, 211, 213, 21211, 21213 etc. Since L_a and L_b contain only words starting with 1, it is obvious that they are subsets of L_e . Moreover, $L_b = 1L_e$ and $L_a = 1L_e \cup 1L_b$ so $L_b \subset L_e$ implies $L_a = L_b$. It seems interesting that even this simple example leads to questions on regular languages.

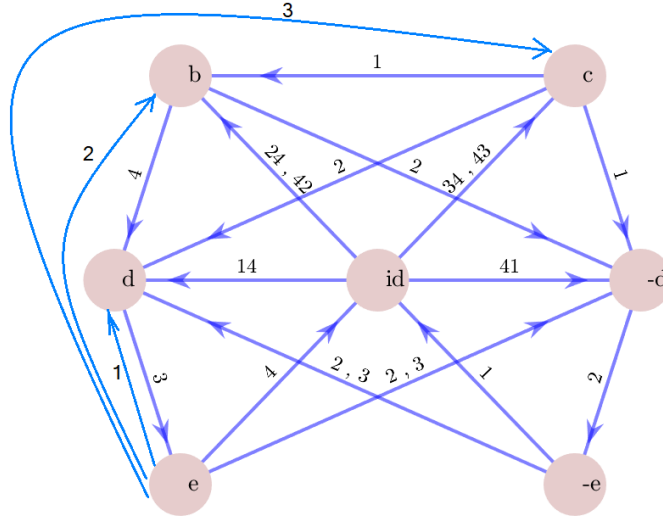


Figure 8: Another overlap graph for which the GIFS can be determined manually. Some edges not needed for the calculation were left, for better visibility.

8 Another detailed example

The overlap graph in Figure 8 describes an example with $m = 4$ maps where the overlaps are more separated. We determine $S_k, k = 2, \dots, m$ according to (10). For $k = 2, 3$ we find no edges with label 21, 31 or 32. Thus the second and third piece obtain the names $S_1 = \emptyset$ and $B_1 = A$ after renumbering. The symbols S_2, B_2 are needed only for $k = 4$ where we have three edges and $S_2 = \{b, c, -d\}$:

$$B_1 = f_1(B_1) \cup f_2(B_1) \cup f_3(B_1) \cup f_4(B_2).$$

Next, we determine the equation for B_2 . From S_2 , outgoing edges with label 1 lead to b and $-d$. We have a new overlap set $S_3 = S_{1,2} = \{b, -d\}$ and a corresponding attractor B_3 . Similarly, outgoing edges from S_2 with label 2 lead to $S_4 = S_{2,2} = \{d, -d, -e\}$. With label 3, however, there are no edges from S_2 , so $S_{3,2} = \emptyset = S_1$. For label 4, we have the overlaps of $S_2 = \{b, c, -d\}$ and d which is approached by an edge from b . With $S_5 = \{b, c, d, -d\}$, the equation for B_2 is

$$B_2 = f_1(B_3) \cup f_2(B_4) \cup f_3(B_1) \cup f_4(B_5).$$

For B_3 with $S_3 = \{b, -d\}$, the pieces 3,4 are the same. But for label 1, no edge can be found, and for label 2, we get the new overlap set $S_6 = \{-d, -e\}$:

$$B_3 = f_1(B_1) \cup f_2(B_6) \cup f_3(B_1) \cup f_4(B_5).$$

We continue with the successor vertices of $S_4 = \{d, -d, -e\}$. For label 1, the successor of $-e$ is id so that the first term of the equation for B_4 vanishes. Label 4 leads to B_2 , and for labels 2

and 3, we get new sets: $S_7 = \{d, -e\}$ and $S_8 = \{d, e\}$:

$$B_4 = f_2(B_7) \cup f_3(B_8) \cup f_4(B_2) .$$

For $S_5 = \{b, c, d, -d\}$ we get a similar equation as for $S_2 = \{b, c, -d\}$. The only difference is the edge from d to e with label 3 which leads to $S_9 = \{e\}$ and

$$B_5 = f_1(B_3) \cup f_2(B_4) \cup f_3(B_9) \cup f_4(B_5) .$$

Now we can state some properties of the equations. The first term vanishes if S_k contains $-e$, the last term disappears when S_k contains e . If the last term does not disappear, it will be $f_4(B_5)$ in case S_k contains b , else $f_4(B_2)$. In this way, we derive the equations

$$B_6 = f_2(B_7) \cup f_3(B_{10}) \cup f_4(B_2) \quad \text{with } S_{10} = \{d\} , \quad B_7 = f_2(B_{10}) \cup f_3(B_8) \cup f_4(B_2) .$$

For $S_8 = \{d, e\}$ we get new sets $S_{1,8} = \{d\} = S_{10}$ and $S_{3,8} = \{c, -d, e\} = S_{11}$ and the old set $S_{2,8} = \{-d, b\} = S_3$. The last term disappears:

$$B_8 = f_1(B_{10}) \cup f_2(B_3) \cup f_3(B_{11}) .$$

Similar results are obtained for $S_9 = \{e\}$, only with the new set $S_{12} = \{c, -d\}$ for $i = 3$. The remaining equations are

$$B_9 = f_1(B_{10}) \cup f_2(B_3) \cup f_3(B_{12}) , \quad B_{10} = f_1(B_1) \cup f_2(B_1) \cup f_3(B_9) \cup f_4(B_2) ,$$

$$B_{11} = f_1(B_{13}) \cup f_2(B_{14}) \cup f_3(B_{12}) , \quad B_{12} = f_1(B_3) \cup f_2(B_7) \cup f_3(B_1) \cup f_4(B_2) ,$$

$$B_{13} = f_1(B_1) \cup f_2(B_6) \cup f_3(B_9) \cup f_4(B_5) , \quad B_{14} = f_2(B_4) \cup f_3(B_8) \cup f_4(B_5) .$$

After establishing the GIFS equations, let us consider the IFS in the complex plane. It is derived from the expanding map $g(z) = 2iz$, with translations and point reflections as ‘digits’:

$$f_1(z) = \frac{-i}{2}z - 1 - 2i , \quad f_2(z) = \frac{i}{2}z + 1 - 2i , \quad f_3(z) = \frac{i}{2}z - 2 + i , \quad f_4(z) = \frac{-i}{2}z + 1 .$$

The IFS fulfils the weak separation condition since the expanding factor $2i$ is a complex Pisot number [6]. The attractor A in Figure 9 can be considered as an overlapping and asymmetric modification of the 2×2 square [10]. The overlaps all occur with piece A_4 , while A_1 meets A_2 as well as A_3 in two points only. The overlaps between A_4 and A_2 as well as A_3 correspond to neighbor maps which are point reflections: $b(z) = -z + 4$, $c(z) = -z - 2 - 6i$. The overlap between A_1 and A_4 , and between second-level pieces A_{13} and A_{42} , is given by the translations $d(z) = z - 4 + 4i$, $e(z) = z + 2 + 2i$, respectively. It is correct to write $-d, -e$ for the inverse translations. Figure 9 shows the different types of overlaps in the neighbourhood of a certain piece. The attractor B_1 of the constructed GIFS is drawn on level 2, so that the shape of B_2 (red), B_3 (green), B_4 (turquoise), and B_5 (green) are visible. The other pieces are copies of B_1 (white, yellow, blue, purple). In the view of the fractal tiling on the bottom right, most of the attractors B_k are represented.

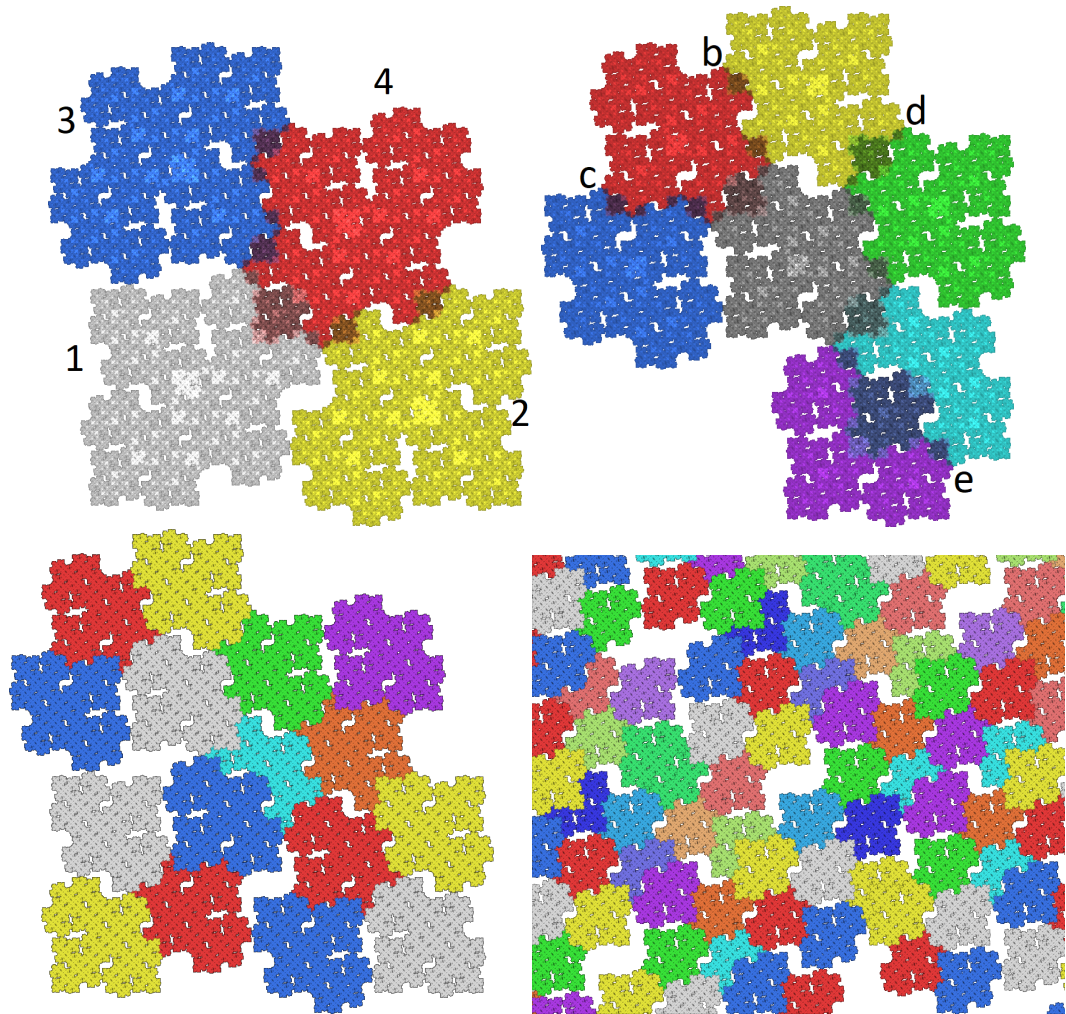


Figure 9: Top: the attractor A and its overlaps in the neighborhood of a piece. Bottom: the GIFS attractor B_1 on level 2 and a close-up of the fractal tiling generated by the GIFS.

When we tested the method with the reverse ordering of mappings, starting with $S_1 = \{d\}$, $S_2 = \{b\}$, and $S_3 = \{c\}$, we obtained 17 GIFS attractors. The dimension of the attractors B_k is of course the same, $\beta = \log \lambda / \log 2 \approx 1.9364$ where λ is the spectral radius of the $n \times n$ incidence matrix S of the B_k . The matrices have characteristic polynomials with different degree n , but both contain the minimal polynomial $\lambda^5 - 4\lambda^4 - 2\lambda^3 + 9\lambda^2 + 4\lambda + 2$ of λ as a factor.

9 Computational problems

Larger examples are better proceeded by computer. The GIFS algorithm was implemented in MATLAB and checked for various IFS. In all cases, the computer-generated GIFS formally

fulfilled Theorem 1. However, our algorithm does not minimize the number of GIFS attractors, due to the very special form (3) of the equations. In Figure 10, for instance, equivalence of attractors is up to translation. So the four congruent pieces of the picture in the middle are different attractors. Even the translations have a special form so that the two types of triangles visible in the picture on the right represent four attractors.

It is a mathematical problem to find all possible GIFS representations of some attractor B_1 , or at least a minimal one. Our examples indicate that in more complicated examples there are often many GIFS representations. For self-similar sets with the OSC, however, the existence of two truly different IFS representations is rather an exception.

Our computer experiments also led to computational problems. The algorithm can produce many unnecessary sets B_k and networks of equations for hidden duplicates. It can happen that two vertices of the overlap graph represent the same overlap, as v and w in Figure 3 or a and b in Figure 6. A more frequent case is that the overlap of one vertex s is contained in the overlap given by another vertex t , as was explained in Section 7 in terms of the regular languages L_s . This happened also in Figure 8 where $L_e = 4 \cup 22L_{-e} \cup 32L_{-e}$ and $L_b = 43L_e \cup 22L_{-e}$ implies $A \cap b(A) \subset A \cap e(A)$. So $S = \{e\}$ and $S = \{e, b\}$ would describe the same attractor. Fortunately, the S_k in this example were not concerned.

In larger examples, the sets S_k may contain more than 10 vertices, and the question then is whether the language L_s for some vertex s is contained in the large language generated by all vertices of S_k . In automata theory, various algorithms have been developed for such problems [16]. The challenge is to give an efficient implementation of a suitable method for our purpose.

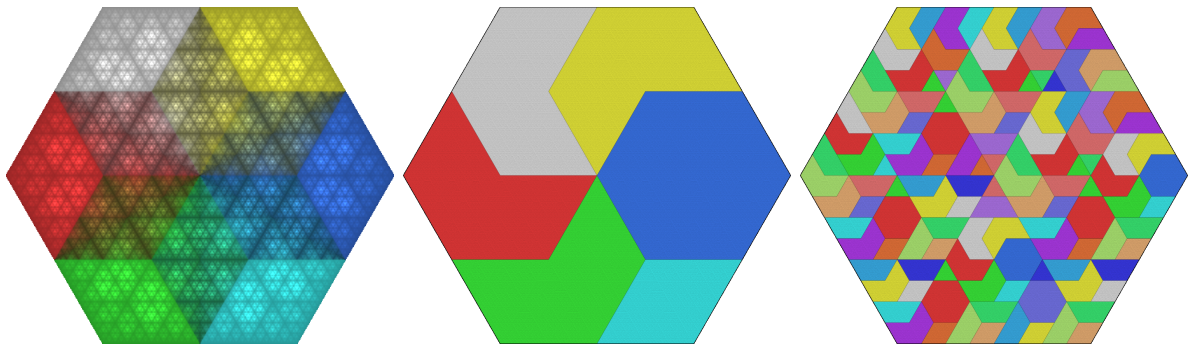


Figure 10: Left: the hexagon as overlapping attractor. The mappings are $f_k(z) = \frac{z}{2} + \omega^{k-1}$, $k = 1, \dots, 6$ where $\omega = \frac{1}{2}(1 + i\sqrt{3})$ fulfils $\omega^6 = 1$. Middle and right: the GIFS representation of B_1 on level 1 and level 3.

In the overlapping hexagon of Figure 10 the overlaps are rhombs. Let us number them cyclically 1,...,6. Overlaps 1 and 2 together form a trapezium, half of a hexagon. The B_k generated by the overlaps 1,2,4,5 should then be empty since the overlaps cover the whole hexagon. However, the algorithm does not recognize this fact and establishes an equation. The GIFS solution for this B_k becomes an interval – the diameter between the two halves – which then appears as part of other B_j . The overlaps 1,3,5 also cover the hexagon but do not generate such a phantom attractor. Three of 18 attractors were intervals and thus superficial.

From a theoretical viewpoint, such lower-dimensional attractors are interesting since they are not detected by regular languages. We need the infinite sequences of addresses to verify that the overlaps 1,2,4,5 really cover the hexagon. However, from a practical viewpoint lower-dimensional attractors are easy to remove. We just take the irreducible part of the incidence matrix S of the B_k .

For the two examples of the next section, it was enough to adopt a heuristical strategy: take the irreducible part, order the matrix of equations so that identical equations stand next to each other, remove all but one of a group of identical attractors, rename their appearance in other equations, renumber the remaining sets and equations and try to repeat the whole procedure. This was not sufficient for more complicated examples. Even for a WSC Cantor set with only 37 overlaps, after reducing the number of equations from 240 to 185, we are not sure that further reduction is impossible. More systematic computer work is necessary to treat such cases.

10 Self-replicating tilings

If the self-similar set A has non-empty interior, it is called a tile. By repeated application of f^{-1} with $f \in F^*$ and fixed point in the interior, we generate a covering of \mathbb{R}^d . Our GIFS will turn this covering into a proper tiling. Such tilings are known as self-replicating or self-similar tilings [33, 51], and there is an extensive literature, see for instance [27, 48]. Well-known examples are the aperiodic tilings by Robinson, Penrose, and Ammann [4], [28, Chapter 11]. Other examples, first treated by Rauzy, are obtained from substitutions with a Pisot eigenvalue of the incidence matrix [2, 3]. Our algorithm provides an alternative to substitutions and yields new examples. We first construct an overlapping tiling. The finite type property is fulfilled when the expanding factor is complex Pisot and the other data are algebraic integers in the generated number field [6]. We get a covering when the IFS has sufficiently many mappings. Then we construct the GIFS as above.

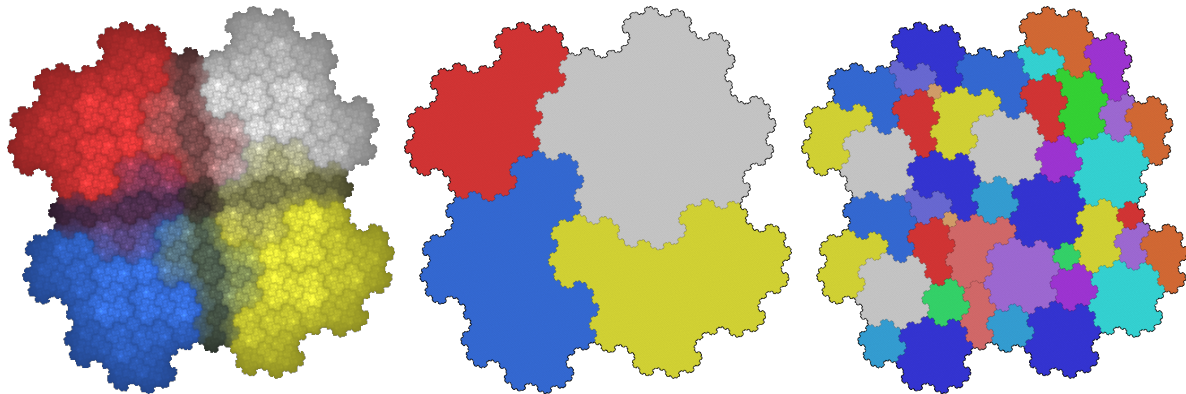


Figure 11: Left: the overlapping tile obtained from a complex Pisot number of degree 4 and translation vectors which form a square. Middle and right: the GIFS representation of B_1 on level 1 and level 3. Thirteen sets B_k are needed.

For an example, we take the complex Pisot number λ with minimal polynomial $p(\lambda) = \lambda^4 + 2\lambda^3 + 4\lambda^2 + 2\lambda + 1$. Since $p(\lambda) = (\lambda^2 + \lambda + 1)^2 + \lambda^2$, we have $\lambda + 1/\lambda + 1 = \pm i$. Thus i is in the generated number field. We choose the IFS $f_k(z) = \frac{z}{\lambda} + v_k$ so that $v_1 = -\lambda, v_2 = i\lambda = 1 + \lambda + \lambda^2, v_3 = \lambda, v_4 = -i\lambda$ form a square with midpoint zero, generating a symmetric attractor. Since $|\lambda| \approx 1.7 < 2$, the formal similarity dimension is $\log 4 / \log |\lambda| > 2.6$ and it is quite plausible that the attractor is a tile, even though there are heavy overlaps.

In this example we have 45 proper neighbor maps from which 29 describe overlaps. The theoretical bound for the number of GIFS attractors is of magnitude 2^{28} . However, the practical situation is much better. The algorithm determined 51 sets B_k , but the irreducible component of B_1 contained only 18 sets. Removing obvious duplicates we arrived at 13 GIFS attractors which are represented in the image on the right of Figure 11. Apparently all B_k are homeomorphic to a disk. They include copies of the symmetric attractor A with four different sizes. Actually, the GIFS system contains three equations with a single term:

$$\begin{aligned} B_1 &= f_1(B_1) \cup f_2(B_2) \cup f_3(B_3) \cup f_4(B_4), & B_2 &= f_1(B_5) \cup f_2(B_6) \cup f_3(B_3) \cup f_4(B_4), \\ B_3 &= f_1(B_1) \cup f_2(B_7) \cup f_3(B_8) \cup f_4(B_4), & B_4 &= f_1(B_1) \cup f_2(B_7), & B_6 &= f_1(B_{10}) \cup f_4(B_9), \\ B_5 &= f_1(B_1) \cup f_2(B_2) \cup f_4(B_9), & B_7 &= f_1(B_{11}) \cup f_2(B_6) \cup f_3(B_3), & B_8 &= f_1(B_{12}) \cup f_2(B_7), \\ B_9 &= f_2(B_7), & B_{10} &= f_1(B_1) \cup f_2(B_2), & B_{11} &= f_4(B_9), & B_{12} &= f_3(B_3) \cup f_4(B_{13}), & B_{13} &= f_1(B_1). \end{aligned}$$

The main factor of the characteristic polynomial of the incidence matrix of the B_k is $x^8 + x^7 - 3x^6 - 15x^5 - 20x^4 - 15x^3 - 3x^2 + x + 1$, and the spectral radius is a real Pisot number, which within numerical accuracy coincides with $|\lambda|^2$, confirming the tiling property.

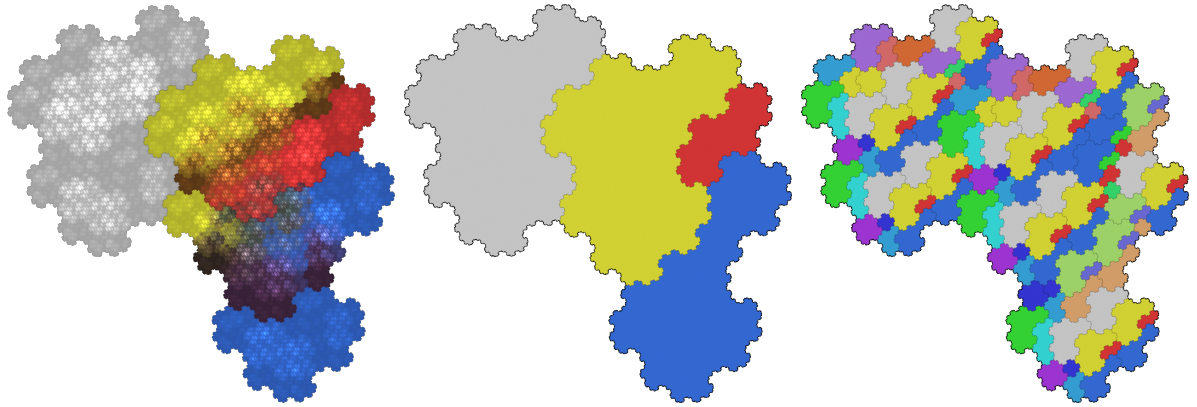


Figure 12: Left: a non-symmetric modification of Figure 11 which admits 67 overlaps and still has only 13 attractors B_k . Middle and right: the GIFS representation of B_1 on level 1 and 4.

Figure 12 shows a non-symmetric example with the same complex Pisot factor. The v_k now are $\lambda, i\lambda - 1, \lambda(1 - i), \lambda^3 + \lambda(1 - i)$. There are 97 proper neighbor maps, among them 67 overlaps. Nevertheless it was possible to reduce the initial number of 87 equations to 13 by taking the irreducible part of the matrix and removing overlaps. Among the 13 attractors, three pairs seem to be translations of each other. Such examples give some hope to get small numbers of equations even for complicated overlap structure.

References

- [1] S. Akiyama. On the boundary of self-affine tilings generated by Pisot numbers. *J. Math. Soc. Japan*, 54(2):283–308, 2002.
- [2] S. Akiyama, M. Barge, V. Berthé, J.-Y. Lee, and A. Siegel. On the Pisot substitution conjecture. In J. Kellendonk, D. Lenz, and J. Savinien, editors, *Mathematics of Aperiodic Order*, volume 309 of *Progress in Mathematics*, pages 33–72. 2015.
- [3] P. Arnoux and S. Ito. Pisot substitutions and Rauzy fractals. *Bull. Belg. Math. Soc. Simon Stevin*, 8(2):181–207, 2001.
- [4] M. Baake and U. Grimm. *Aperiodic Order, Vol. 1: A mathematical invitation*. Cambridge University Press, Cambridge, 2013.
- [5] C. Bandt. Self-similar tilings and patterns described by mappings. In R.V. Moody, editor, *The Mathematics of Long-range Aperiodic Order*, volume C 489 of *NATO ASI Series*, pages 45–84. Kluwer Academic Publishers, 1997.
- [6] C. Bandt. Elementary fractal geometry. 3. Complex Pisot factors imply finite type. *arXiv:2308.16580*, 2023.
- [7] C. Bandt. Elementary fractal geometry. 4. Automata-generated topological spaces. *arXiv:2312.01486*, 2023.
- [8] C. Bandt and S. Graf. Self-similar sets 7. A characterization of self-similar fractals with positive Hausdorff measure. *Proc. Amer. Math. Soc.*, 114:995–1001, 1992.
- [9] C. Bandt, N.V. Hung, and H. Rao. On the open set condition for self-similar fractals. *Proc. Amer. Math. Soc.*, 134:1369–1374, 2005.
- [10] C. Bandt and D. Mekhontsev. Elementary fractal geometry. New relatives of the Sierpiński gasket. *Chaos: An Interdisciplinary Journal of Nonlinear Science*, 28(6):063104, 2018.
- [11] C. Bandt and M. Mesing. Self-affine fractals of finite type. In *Convex and fractal geometry*, volume 84 of *Banach Center Publ.*, pages 131–148. Polish Acad. Sci. Inst. Math., Warsaw, 2009.
- [12] B. Bárány, K. Simon, and B. Solomyak. *Self-similar and self-affine sets and measures*, volume 276 of *Mathematical Surveys and Monographs*. American Mathematical Society, 2023.
- [13] L. Barnsley and M. Barnsley. Central open sets tilings. *arXiv:2111.07530*, 2021.
- [14] L. F. Barnsley and M. F. Barnsley. Blowups and tops of overlapping iterated function systems. *arXiv:2302.10372*, 2023.
- [15] M. Barnsley and A. Vince. Tilings from graph directed iterated function systems. *Geometriae Dedicata*, 212:299–324, 2021.

- [16] J. Berstel, L. Boasson, O. Carton, and I. Fagnot. Minimalisation of automata. In *Handbook of Automata Theory*, pages 337–374. European Mathematical Society, 2021. arXiv:1010.5318.
- [17] C.J. Bishop and Y. Peres. *Fractal sets in probability and analysis*. Cambridge University Press, Cambridge, 2017.
- [18] D. Broomhead, J. Montaldi, and N. Sidorov. Golden gaskets: variations on the sierpiński sieve. *Nonlinearity*, 17:1455–1480, 2004.
- [19] K. Dajani, K. Jiang, D. Kong, W. Li, and L. Xi. Multiple codings of self-similar sets with overlaps. *Advances Applied Math.*, 124:102146, 2021.
- [20] M. Das and G. A. Edgar. Finite type, open set conditions and weak separation conditions. *Nonlinearity*, 24(9):2489, 2011.
- [21] M. Das and G.A. Edgar. Separation properties for graph-directed self-similar fractals. *Topology and its Applications*, 152(1-2):138–156, 2005.
- [22] Juan Deng, Zhiying Wen, and Lifeng Xi. Finite type in measure sense for self-similar sets with overlaps. *Mathematische Zeitschrift*, 298:821 – 837, 2020.
- [23] P. Duvall, J. Keesling, and A. Vince. The Hausdorff dimension of the boundary of a self-similar tile. *J. London Math. Soc.*, 61:748–760, 2000.
- [24] D.B.A. Epstein, J.W. Cannon, D.F. Holt, S.V.F. Levy, M.S. Paterson, and W.P. Thurston. *Word processing in groups*. Jones and Bartlett Pub., London, 1992.
- [25] D.-J. Feng. The topology of polynomials with bounded integer coefficients. *J. Eur. Math. Soc.*, 18:181–193, 2016.
- [26] J. M. Fraser, A. M. Henderson, E. Olson, and J. C. Robinson. On the Assouad dimension of self-similar sets with overlaps. *Advances in Mathematics*, 273:188–214, 2015.
- [27] D. Frettlöh, E. Harriss, and F. Gähler. Tilings encyclopedia. <https://tilings.math.uni-bielefeld.de/>, 2023.
- [28] B. Grünbaum and G.C. Shephard. *Patterns and Tilings*. Freeman, New York, 1987.
- [29] K. E. Hare and A. Rutar. Local dimensions of self-similar measures satisfying the finite neighbor condition. *Nonlinearity*, 35:4876–4904, 2022.
- [30] K.E. Hare, K.G. Hare, and A. Rutar. When the weak separation condition implies the generalized finite type condition. *Proceedings of the American Mathematical Society*, 149(4):1555–1568, 2021.
- [31] J.E. Hopcroft and J. Ullman. *Introduction to automata theory, languages and computation*. Addison-Wesley, 1979.

- [32] A. Käenmäki and E. Rossi. Weak separation condition, Assouad dimension, and Furstenberg homogeneity. *Ann. Acad. Sci. Fenn. Math.*, 41:465–490, 2016.
- [33] R. Kenyon. The construction of self-similar tilings. *Geom. Funct. Anal.*, 6:471–488, 1996.
- [34] S.P. Lalley. β -expansions with deleted digits for Pisot numbers β . *Trans. Amer. Math. Soc.*, 349(11):4355–4365, 1997.
- [35] K.-S. Lau and S.-M. Ngai. Multifractal measures and a weak separation condition. *Advances in Mathematics*, 141:45–96, 1999.
- [36] K.-S. Lau, S.-M. Ngai, and H. Rao. Iterated function systems with overlaps and self-similar measures. *J. London Math. Soc.*, 63(1):99–116, 2001.
- [37] D. Lind and B. Marcus. *An introduction to symbolic dynamics and coding*. Cambridge University Press, 1995.
- [38] B. Loridant. Crystallographic number systems. *Monatsh. Math.*, 167:511–529, 2012.
- [39] B. Loridant and S.-Q. Zhang. Topology of a class of p2-crystallographic replication tiles. *Indagationes Math.*, 28(4):805–823, 2017.
- [40] R.D. Mauldin and S.C. Williams. Hausdorff dimension in graph-directed constructions. *Trans. Amer. Math. Soc.*, 309:811–829, 1988.
- [41] D. Mekhontsev. IFS tile finder, version 2.60. <https://ifstile.com>, 2021.
- [42] P.A.P. Moran. Additive functions of intervals and hausdorff measure. *Math. Proc. Cambridge Phil. Soc.*, 42:15–23, 1946.
- [43] S.-M. Ngai and Y. Wang. Hausdorff dimension of self-similar sets with overlaps. *J. London Math. Soc.*, 63:655–672, 2001.
- [44] N. Nguyen. Iterated function systems of finite type and the weak separation property. *Proc. Amer. Math. Soc.*, 130(2):483–487, 2002.
- [45] A. Pyörälä. The scenery flow of self-similar measures with weak separation condition. *Ergodic Theory and Dynamical Systems*, 42:3167 – 3190, 2021.
- [46] K. Scheicher and J.M. Thuswaldner. Neighbors of self-affine tiles in lattice tilings. In P. Grabner and W. Woess, editors, *Fractals in Graz 2001*, pages 241–262. Birkhäuser, 2003.
- [47] A. Schief. Separation properties for self-similar sets. *Proc. Amer. Math. Soc.*, 122:111–115, 1994.
- [48] B. Solomyak. Delone sets and dynamical systems. *Substitution and Tiling Dynamics: Introduction to Self-inducing Structures: CIRM Jean-Morlet Chair, Fall 2017*, pages 1–32, 2020.

- [49] R.S. Strichartz and Y. Wang. Geometry of self-affine tiles 1. *Indiana Univ. Math. J.*, 48:1–24, 1999.
- [50] A.V. Tetenov and A.K.B. Chand. On weak separation property for affine fractal functions. *Siberian Electr. Math. Rep.*, 12:967–972, 2015.
- [51] W.P. Thurston. Groups, tilings, and finite state automata. AMS Colloquium Lectures, Boulder, CO, 1989.
- [52] J. Thuswaldner and S. Zhang. On self-affine tiles whose boundary is a sphere. *Trans. Amer. Math. Soc.*, 373(1):491–527, 2020.
- [53] Yu-Feng Wu. Matrix representations for some self-similar measures on R^d . *Mathematische Zeitschrift*, 301(4):3345–3368, 2022.
- [54] M.P.W. Zerner. Weak separation properties for self-similar sets. *Proc. Amer. Math. Soc.*, 124:3529–3539, 1996.